BJP BRITISH JOURNAL OF PHARMACOLOGY
BPS BRITISH PHARMACOLOGICAL SOCIETY

BJP British Journal of Pharmacology

DOI:10.1111/j.1476-5381.2010.00897.x
www.brjpharmacol.org

RESEARCH PAPER

Differential effects of K_v11.1 activators on K_v11.1a, K_v11.1b and K_v11.1a/K_v11.1b channels

AP Larsen[1]*, BH Bentzen[1]* and M Grunnet[1,2]

[1]*The Danish National Research Foundation Centre for Cardiac Arrhythmia, Department of Biomedical Sciences, University of Copenhagen, Blegdamsvej 3, Copenhagen N, Denmark, and* [2]*NeuroSearch A/S, Pederstrupvej 93, Ballerup, Denmark*

Correspondence
Morten Grunnet, NeuroSearch A/S, Pederstrupvej 93, DK-2750 Ballerup, Denmark. E-mail: mgr@neurosearch.dk

*These authors contributed equally to the study.

Keywords
Kv11.1a; Kv11.1b; hERG1a; hERG1b; NS1643; RPR260243

Received
20 January 2010
Revised
22 April 2010
Accepted
22 April 2010

BACKGROUND AND PURPOSE

K_v11.1 channels are involved in regulating cellular excitability in various tissues including brain, heart and smooth muscle. In these tissues, at least two isoforms, K_v11.1a and K_v11.1b, with different kinetics, are expressed. K_v11.1 activators are potential therapeutic agents, but their effects have only been tested on the K_v11.1a isoform. In this study, the effects of two different K_v11.1 activators, NS1643 and RPR260243, were characterized on K_v11.1a and K_v11.1b channels.

EXPERIMENTAL APPROACH

K_v11.1a and K_v11.1b channels were expressed in *Xenopus laevis* oocytes, and currents were measured using two-electrode voltage clamp. *I*/*V* curves and channel kinetics were measured before and after application of 30 μM NS1643 or 10 μM RPR260243.

KEY RESULTS

NS1643 increased steady-state currents through Kv11.1b several fold more than through K_v11.1a channels, without affecting EC_{50} values. NS1643 increased activation rates and decreased rates of inactivation, recovery from inactivation and deactivation for both channels. Except for activation, where effect of NS1643 was comparable, relative changes were greater for Kv11.1b than for K_v11.1a. RPR260243 increased steady-state currents only through Kv11.1a channels, but slowed the process of deactivation for both channels primarily by decreasing time constant of slow deactivation. This effect was greater on K_v11.1b than on K_v11.1a. Effects of both compounds on heteromeric K_v11.1a/K_v11.1b channels were similar to those on K_v11.1a.

CONCLUSIONS AND IMPLICATIONS

Both NS1643 and RPR260243 displayed differential effects on K_v11.1a and K_v11.1b channels, the effects being relatively more pronounced on K_v11.1b channels. This affirms the importance of testing the effect of K_v11.1 activators on different channel isoforms.

Abbreviations

I_{Kr}, the rapid component of the delayed-rectifier potassium channel; *I*/*V*, current/voltage; K_v, voltage-gated potassium channel

Introduction

Potassium currents carried by the K_v11.1 (ether-a-go-go-related gene or ERG1) ion channel affect excitability in a range of tissues including brain (Chiesa *et al.*, 1997; Huffaker *et al.*, 2009), heart (Sanguinetti *et al.*, 1995) and smooth muscle cells (Ohya *et al.*, 2002; Farrelly *et al.*, 2003). In these tissues, at least two different isoforms of K_v11.1, namely K_v11.1a and K_v11.1b, have been found to be co-expressed (Ohya *et al.*, 2002; Jones *et al.*, 2004; Guasti *et al.*, 2005). K_v11.1a is the full-length isoform originally

characterized (Sanguinetti *et al.*, 1995; Trudeau *et al.*, 1995), and $K_v11.1b$ is an N-terminal splice variant (Lees-Miller *et al.*, 1997; London *et al.*, 1997). Specifically, compared to $K_v11.1a$, the N-terminal of $K_v11.1b$ is 340 amino acids shorter. However, the initial 36 amino acids of $K_v11.1b$ are unique to this isoform. Furthermore, the two isoforms differ in their kinetic gating profiles. $K_v11.1b$ displays faster kinetics of activation, recovery from inactivation and most prominently deactivation as compared to $K_v11.1a$ (Larsen *et al.*, 2008).

Recently, $K_v11.1$ activators have gained interest as potential therapeutic agents mainly as a potential treatment of certain types of cardiac arrhythmias (Kang *et al.*, 2005; Zhou *et al.*, 2005; Hansen *et al.*, 2006a,b; 2007; Diness *et al.*, 2008). Two of these compounds have markedly different modes of action. NS1643 has been shown to increase $K_v11.1$ currents primarily by right-ward shifting the inactivation curve and by slowing the fast inactivation process (Casis *et al.*, 2006; Hansen *et al.*, 2006a), although effects on other kinetic parameters have also been described (Xu *et al.*, 2008). In contrast, RPR260243 almost exclusively acts by slowing the deactivation process of the channels (Kang *et al.*, 2005). However, these compounds have only been characterized on the $K_v11.1a$ isoform. In the heart, both $K_v11.1a$ and $K_v11.1b$ have been shown to contribute to the generation of I_{Kr}, the rapid delayed rectifier current (Jones *et al.*, 2004). The functional properties of I_{Kr} have recently been suggested to depend on the relative abundance of the $K_v11.1$ isoforms (Larsen and Olesen, 2010). Furthermore, alterations in the relative expression of $K_v11.1$ isoforms in neurones have been linked to schizophrenia (Huffaker *et al.*, 2009). Thus, it is clear that $K_v11.1$ isoforms other than $K_v11.1a$ contribute to the physiological function of $K_v11.1$-mediated currents. Given the inherent kinetic differences between the $K_v11.1a$ and b isoforms (Larsen *et al.*, 2008), it is likely that activators that affect specific kinetic properties of the channels will display differential effects on the $K_v11.1$ isoforms. Such differential activators may prove valuable tools to address the physiological role of $K_v11.1$ isoforms in a given tissue. Additionally, given the therapeutic potential of $K_v11.1$ activators, it is important to investigate possible differential effects of the compounds on the $K_v11.1$ isoforms.

Here, we tested the effects of the $K_v11.1$ channel activators NS1643 and RPR260243 on the human variants of the $K_v11.1a$ and $K_v11.1b$ isoforms. Also, we tested their effects on both homomeric and heteromeric channels. Our results demonstrate that both activators have differential effects on $K_v11.1$ channels depending on the subunit composition, and suggest that it may be possible to differentially target $K_v11.1$ isoforms. Thus, our results affirm the importance of testing the effect of $K_v11.1$ activators on different channel isoforms.

Methods

All animal procedures conformed to the guidelines of the Danish National Committee for Animal Studies. Unless otherwise mentioned, all chemicals were obtained from Sigma-Aldrich (St Louis, MO, USA). The nomenclature of ion channels used in this paper conforms to the standards outlined in Alexander *et al.* (2008).

DNA constructs

cDNAs encoding human $K_v11.1a$ (acc. number NM_000238) and $K_v11.1b$ (acc. number NM_172057) were inserted into pXOOM for expression in *Xenopus laevis* oocytes (Jespersen *et al.*, 2002). The $K_v11.1b$ clone was obtained from A. Arcangeli (Università degli Studi di Firenze, Florence, Italy).

Expression in X. laevis *oocytes*

Preparation and injection of cRNA in XO were performed as previously described (Larsen *et al.*, 2008). Oocytes were injected with 1.25–5 ng of cRNA. For co-expression of $K_v11.1a$ and $K_v11.1b$, cRNAs were mixed in a molar ratio of 4:1 ($K_v11.1a$: $K_v11.1b$) before injection. Experiments were performed 3 days after injection.

Electrophysiological recordings

Measurements on *X. laevis* oocytes were performed with the two-electrode voltage clamp technique using a Dagan CA-1B amplifier (Minneapolis, MN, USA). All recordings were performed at room temperature (21–22°C) under continuous superfusion with Kulori solution (in mM: 87 NaCl, 4 KCl, 1 $MgCl_2$, 1 $CaCl_2$, 5 HEPES, pH 7.4). Oocytes were placed in a perfusion chamber connected to a multibarrel flow system that allowed for rapid change between solutions. Glass pipettes for recording electrodes were pulled from borosilicate glass capillaries (Module Ohm, Herlev, Denmark) on DMZ Universal Puller (Zeitz Instruments, Munich, Germany), and had a tip resistance between 0.5 and 2.5 MΩ when filled with 2 M KCl. The series resistance was compensated using the internal compensatory circuit on the amplifier. Data acquisition was performed with the Pulse software (HEKA Elektronik, Lambrecht/Pfalz, Germany). For all recordings, the holding potential was –80 mV. The time interval between recordings was adjusted depending on the specific

protocol and the drug applied in order to allow channels to fully deactivate before a new protocol was initiated.

Data analysis was performed with Igor Pro (Wavemetrics, Lake Oswego, OR, USA) and GraphPad Prism (GraphPad Software Inc, San Diego, CA, USA). *I/V* curves were constructed by measuring the current at the end of a 2 s voltage step to potentials ranging from –80 to +40 mV. The data were plotted against the corresponding membrane potentials. Similarly, the peak tail currents, measured at –60 mV following the depolarizing step, were plotted against the membrane potential of the depolarizing step to construct the activation curves. A Boltzmann function ($I/I_{max} = I_{min} + (I_{max} - I_{min})/\{1 + \exp[(V_{50} - V)/k)]\}$ was fitted to the activation curves to obtain the potential of half-maximal activation (V_{50}) and the slope factor (k). The time constant of activation (τ_{act}) at 0 mV was determined using the standard envelope of tails protocol, measuring the peak tail current at either –60 or –100 mV. A mono-exponential function was fitted to the normalized peak tail currents to obtain τ_{act}. An estimate of the values of the time constants of channel deactivation (τ_{slow} and τ_{fast}) was obtained by fitting a double-exponential function to tail current traces measured at –60 mV following a voltage step to +40 mV for 1 s to achieve maximal activation. Similarly, the time constant of recovery from inactivation (τ_{rec}) at –60 mV was determined by subtracting the extrapolated fit of the deactivation process from the initial rising phase of the tail currents. The difference between the extrapolated values and the recorded current values represents the time-course of recovery from inactivation. The time constant of this process was estimated by fitting a mono-exponential function to the resulting curve. Inactivation was addressed by first clamping the oocytes at +40 mV for 1 s, then briefly at –120 mV to allow channels to recover from the inactivated state, and finally at 0 mV to investigate the time-course of inactivation at this potential. To avoid significant closure of the channels during the clamp at –120 mV, this step lasted 10 ms for K_v11.1a and 5 ms for K_v11.1b, due to the faster deactivation kinetics of K_v11.1b.

The time constant of inactivation was estimated by fitting a mono-exponential function to the initial steep decrease in current amplitude at 0 mV.

Drugs

NS1643 [1,3-*bis*-(2-hydroxy-5-trifluoromethyl-phenyl)-urea; Hansen *et al.*, 2006a] and RPR260243 [(3*R*,4*R*)-4-[3-(6-methoxyquinolin-4-yl)-3-oxo-propyl]-1-[3-(2,3,5-trifluoro-phenyl)-prop-2-ynyl]-piperidine-3-carboxylic acid; Kang *et al.*, 2005] were synthesized at NeuroSearch A/S, Ballerup, Denmark. The synthesis of RPR260243 was complicated involving more than 10 steps and a very low yield in the final purification step. Therefore, we were only able to obtain limited amounts of RPR260243, and consequently we were not able to do a full set of experiments, including a full concentration–response curve, with this drug. NS1643 was dissolved as a 30 mM stock solution in DMSO. RPR260243 was dissolved as a 10 mM stock solution in DMSO. Both compounds were diluted in the Kulori solution to achieve the desired working concentrations.

Data analysis

Data are represented as mean ± SEM, unless otherwise indicated. Paired *t*-tests or ANOVA followed by Tukey's method of multiple comparisons were used as appropriate to compare data before and after drug application, as well as the relative effects of the compounds on K_v11.1a and K_v11.1b. *P* values below 0.05 were considered statistically significant.

Results

K_v11.1a and K_v11.1b channels were expressed as homomeric or heteromeric K_v11.1a/K_v11.1b (4:1) channels in *X. laevis* oocytes. A molar ratio of 4:1 reflects the apparent ratio of the isoforms as determined by real-time PCR of amplified mRNA in adult human heart (Larsen *et al.*, 2008). To verify that co-expression of K_v11.1a and K_v11.1b led to the formation of heteromeric channels, deactivation kinetics were compared to those of homomeric K_v11.1a and K_v11.1b. Using the average time constants for the deactivation process under control conditions (Figures 3 and 7), the observed current decay for K_v11.1a/K_v11.1b (4:1) was compared to the expected theoretical current decay, assuming the formation of only homomeric channels. The theoretical current decay was calculated as a weighted algebraic summation (4:1) of the deactivation kinetics of K_v11.1a and K_v11.1b homomeric channels. Supporting Information Figure S1 shows the normalized decay of both the observed and theoretical situations. In the observed situation, the current decay was faster than in the theoretical situation. Thus, the observed currents cannot be explained by the presence of homomeric channels only. This argument is valid under the assumption that the expression level is comparable for homomeric K_v11.1a and K_v11.1b channels. The majority of the experiments in this study were not designed to compare current density *per se*; however, statistical comparison of a separate set of experiments, where oocytes were

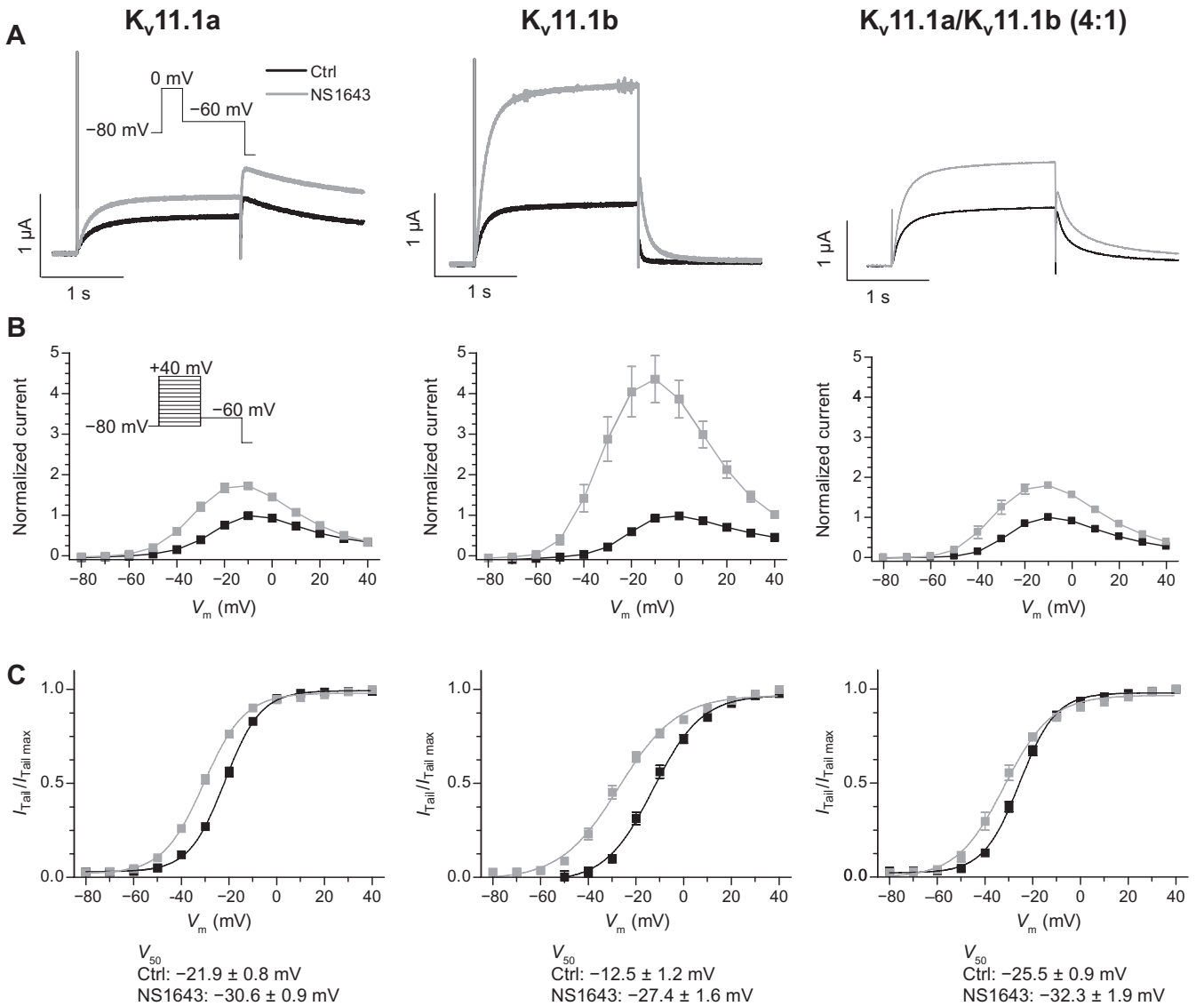

Figure 1

Effect of NS1643 on current–voltage relationships of $K_v11.1$ channels. (A) Representative current traces recorded at a test potential of 0 mV from *Xenopus laevis* oocytes expressing either $K_v11.1a$ (left panel), $K_v11.1b$ (middle panel) or $K_v11.1a/K_v11.1b$ (4:1) (right panel) in the absence and presence of 30 µM NS1643. To construct current–voltage (*I*/*V*) relationships, currents were elicited using the voltage clamp protocol shown in the insert (A). Steady-state currents measured at the end of each step were normalized to the maximum current in control condition, and plotted as a function of the test potential (B). Voltage dependence of activation was investigated by plotting the normalized peak tail current measured immediately after stepping back to –60 mV against the preceding step potential. V_{50} values were calculated from individual Boltzmann fits to the normalized tail current–voltage relationships (C) ($K_v11.1a$; $K_v11.1b$; $K_v11.1/K_v11.1b$: n = 10; 13; 7).

injected with the same amount of either $K_v11.1a$ or $K_v11.1b$ cRNA, showed that the steady-state current measured at the end of a 2 s depolarizing pulse to 0 mV was significantly lower for $K_v11.1b$ than for $K_v11.1a$ homomeric channels ($K_v11.1a$, I = 1.5 ± 0.3 µA, n = 6; $K_v11.1b$, I = 0.6 ± 0.05 µA, n = 9; P < 0.05). If these data were incorporated in the calculation of theoretical current decay, the properties of $K_v11.1a$ homomeric channels would be even more dominant. Thus, the comparison of theoretical and observed current decay clearly demonstrates the existence of functional heteromeric channels. This is in line with previous observations on the formation of heteromeric $K_v11.1a$ and $K_v11.1b$ channels in oocytes (London *et al.*, 1997).

Effects of NS1643 on Kv11.1 channels

The effects of 30 µM NS1643 on steady-state and tail currents were investigated. In Figure 1A, representative current recordings from oocytes expressing $K_v11.1a$ (left side), $K_v11.1b$ (middle) and $K_v11.1a/K_v11.1b$ (right side) channels clamped at 0 mV for

2 s, and then at –60 mV for 2 s under control conditions and after application of NS1643 are shown. The data demonstrate that while NS1643 increased the steady-state current for both K_v11.1 homomeric and heteromeric channels, the increase was more noticeable for K_v11.1b at 0 mV. In Figure 1B, the *I*/*V* relationships are shown for K_v11.1a (left), K_v11.1b (middle) and K_v11.1a/K_v11.1b (right side). The protocol used to determine the *I*/*V* relationship is shown in the inset in Figure 1B. The current amplitude at the end of the 2 s voltage step was plotted against the command potential. For comparison, the data were normalized to the maximum current amplitude under control conditions. NS1643 consistently increased currents through both channels for voltages above –50 mV. The data show that the effect of NS1643 on steady-state current amplitude was greater on K_v11.1b channels over this voltage range. To determine the half-maximal voltage of activation (V_{50}), Boltzmann functions were fitted to the normalized tail current amplitudes measured at –60 mV (Figure 1C). For K_v11.1a (left side), NS1643 shifted the V_{50} value from –21.9 ± 0.8 to –30.6 ± 0.9 mV ($P < 0.05$). For K_v11.1b (middle), NS1643 shifted the V_{50} value from –12.5 ± 1.2 to –27.4 ± 1.6 mV ($P < 0.05$). For heteromeric channels, application of NS1643 shifted the V_{50} value from –25.5 ± 0.9 to –32.3 ± 1.9 mV ($P < 0.05$).

To determine whether differences in the potency of NS1643 could account for the more noticeable effect on K_v11.1b, concentration–response curves were constructed for both isoforms (Supporting Information Figure S2). There was no significant difference between the EC_{50} values for NS1643 on K_v11.1a (9.4 ± 1.1 μM) and K_v11.1b (8.6 ± 0.7 μM).

The effect of NS1643 on activation kinetics at 0 mV was evaluated using an envelope of tails protocol (Figure 2). The protocol was carried out by activating channels at 0 mV for various durations of time (from 10 to 1000 ms), and then measuring the tail current at either –60 or –100 mV. The amplitude of the tail current represents the relative amount of activated channels released from inactivation at a given time-point. The protocols (inset) along with representative current recordings from oocytes expressing K_v11.1a (left side), K_v11.1b (middle) and K_v11.1a/K_v11.1b (right side) are shown in Figure 2A. For simplicity, only currents under control conditions are shown. In Figure 2B, the peak tail currents normalized to maximum amplitude are shown as a function of the duration of the activating step. The solid lines correspond to mono-exponential fits to the data. The data show that NS1643 accelerates activation (decreases τ) of K_v11.1a, K_v11.1b and K_v11.1a/K_v11.1b (4:1) channels. The time constant of activation (τ_{act}) was obtained from the fitted functions, and quantified in Figure 2C. The τ_{act} for the K_v11.1a, K_v11.1b and K_v11.1a/K_v11.1b channels was significantly decreased by NS1643. The relative change in τ_{act} was comparable for Kv11.1a, Kv11.1b and K_v11.1a/K_v11.1b as shown in Figure 2C, demonstrating no differential effect of NS1643 on this parameter.

The deactivation kinetics were determined at –60 mV. In Figure 3A, representative current recordings are shown for K_v11.1a (left side), K_v11.1b (middle) and K_v11.1a/K_v11.1b (right side) before and after application of NS1643. Also shown are enlargements of the tail currents normalized to the peak tail current to allow comparison of the time-course of deactivation. NS1643 slowed the deactivation time-course of both channel isoforms. However, due to the intrinsic fast deactivation of K_v11.1b, the effect is relatively more pronounced on this channel isoform. By fitting a double-exponential function to the current traces, the two time constants of deactivation and their relative contribution to the process could be determined. On K_v11.1a, NS1643 did not significantly change the slow time constant of deactivation (τ_{slow}), whereas on K_v11.1b and K_v11.1a/K_v11.1b, τ_{slow} was increased significantly ($P < 0.001$) as shown in Figure 3B (left side). As shown in Figure 3C (left side), the fast time constant of deactivation (τ_{fast}) was significantly increased by NS1643 for K_v11.1a ($P < 0.05$), K_v11.1b ($P < 0.001$) and K_v11.1a/K_v11.1b ($P < 0.01$). However, comparison of the relative change in τ_{fast} revealed that the effect was greater on K_v11.1b as compared to K_v11.1a and K_v11.1a/K_v11.1b ($P < 0.001$, Figure 3C, right side). The relative contribution of the fast component of deactivation was not changed by NS1643 for K_v11.1a. For K_v11.1b and K_v11.1a/K_v11.1b, the relative contribution of the fast component was significantly decreased by NS1643 ($P < 0.001$ and $P < 0.01$ respectively). Quantification of the relative changes in all three parameters clearly demonstrates that the effects of NS1643 on deactivation kinetics are isoform dependent (K_v11.1a vs. K_v11.1b: $P < 0.01$ for τ_{slow}, $P < 0.001$ for τ_{fast}, $P < 0.05$ for the relative contribution; K_v11.1b vs. K_v11.1a/K_v11.1b: $P < 0.001$ for τ_{fast}; Figure 3B–D, right side). Thus, NS1643 slows deactivation of K_v11.1b relatively more than deactivation of K_v11.1a and K_v11.1a/K_v11.1b.

Inactivation properties were addressed using a three-pulse protocol designed to isolate the process of inactivation (see Methods and inset in Figure 4A for details). In Figure 4A, representative current recordings of K_v11.1a (left side), K_v11.1b (middle) and K_v11.1a/K_v11.1b (right side) channels using such a protocol are shown. The currents have been enlarged and normalized to maximum amplitude for comparison of the time-course of inactivation.

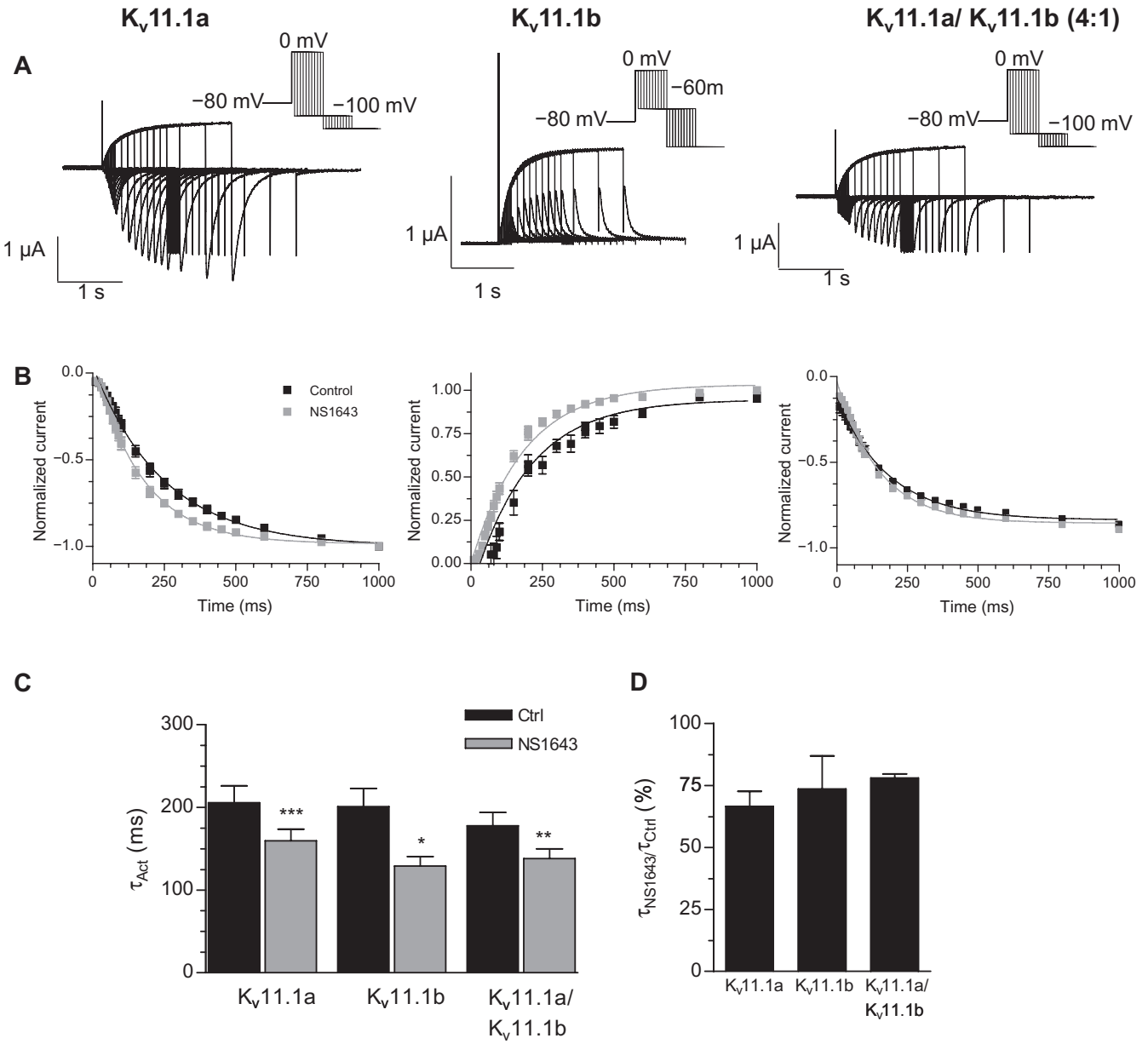

Figure 2

Effect of NS1643 on activation kinetics of K_v11.1 channels. To avoid contribution from fast inactivation, an envelope of tails voltage clamp protocol (insert) was used to study the activation kinetics of K_v11.1a (left panel), K_v11.1b (middle panel) or K_v11.1a/K_v11.1b (4:1) (right panel). Representative current traces are depicted in (A). Peak currents measured when stepping back to –100 mV (K_v11.1a and K_v11.1a/K_v11.1b) or –60 mV (K_v11.1b) were normalized and plotted as a function of activation time. Mean time constants from single exponential fits to the current–time relationships before and after application of 30 µM NS1643, and the relative effect of NS1643 on the time constants for K_v11.1a, K_v11.1b and K_v11.1a/K_v11.1b are shown in (C) and (D). (K_v11.1a; K_v11.1b; K_v11.1a/K_v11.1b: n = 10; 9; 7).

For both homomeric and heteromeric channels, NS1643 slows the process of inactivation as compared to control. Quantification of the time constant of inactivation (τ_{inact}) shows that NS1643 increases τ_{inact} significantly ($P < 0.001$ for both K_v11.1a, K_v11.1b and K_v11.1a/K_v11.1b). However, comparison of the relative change in τ_{inact} shows that the effect is greater on K_v11.1b channels as compared to K_v11.1a or K_v11.1a/K_v11.1b ($P < 0.001$ and $P < 0.001$, respectively, Figure 4C).

The process of recovery from inactivation can be addressed by looking at the initial rising phase of the tail currents after a depolarizing pulse. The data obtained using the deactivation protocol (see above) were used to address the time-course of recovery from inactivation at –60 mV. In Figure 5A,

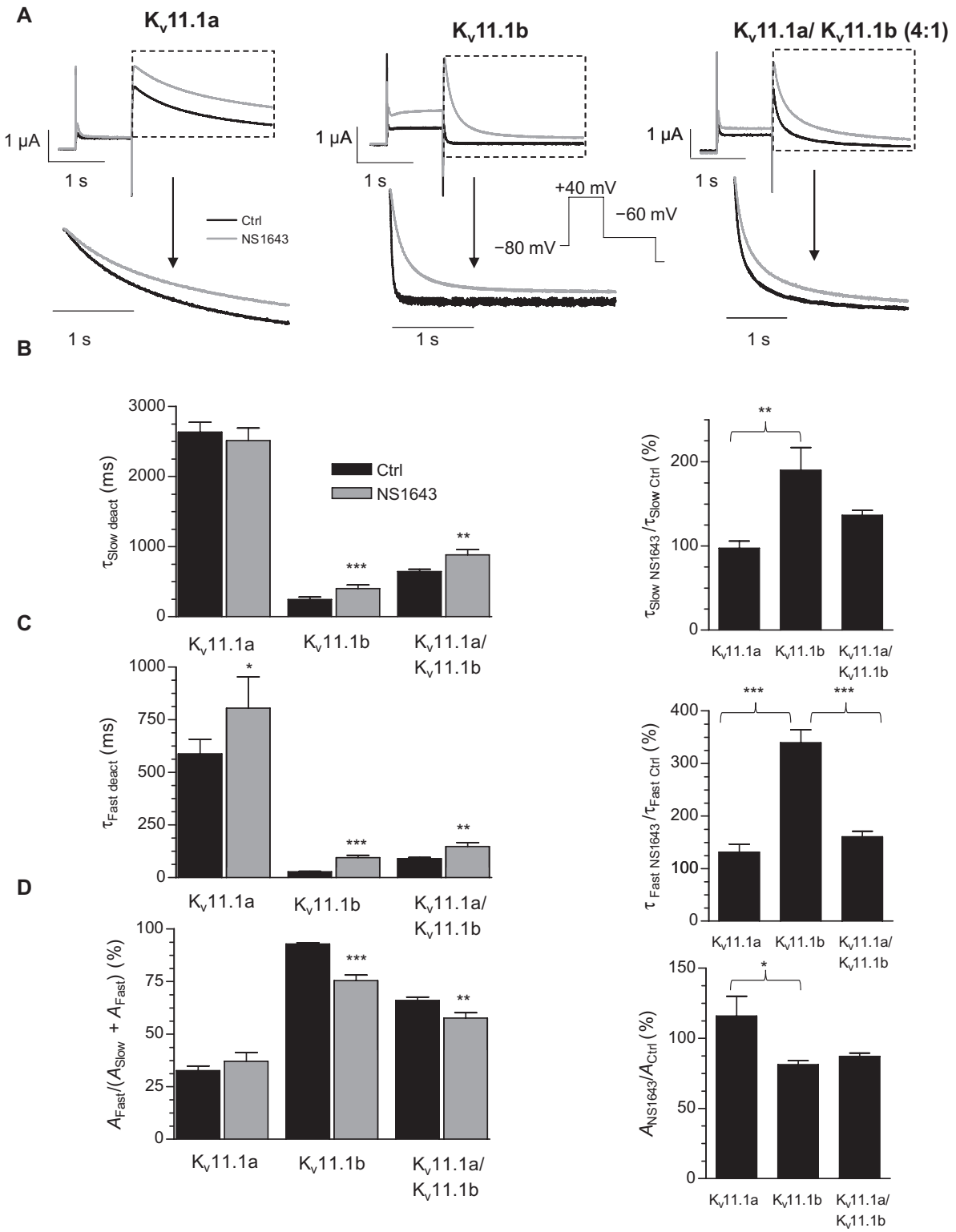

Figure 3

Effect of NS1643 on deactivation kinetics of $K_v11.1$ channels. (A) Representative current traces from oocytes expressing $K_v11.1a$ (left panel), $K_v11.1b$ (middle panel) or $K_v11.a/K_v11.1b$ (4:1) (right panel) in the absence and presence of NS1643, and an enlargement of the tail currents (normalized to maximum current amplitude). Currents were elicited by the voltage clamp protocol shown in the insert in (A). The time-course of deactivation could be described by a double-exponential function. Time constants of the slow component (B), fast component (C) and the relative contribution of the fast and slow component (D) before and after application of 30 µM NS1643 are shown. In addition, the relative effect of NS1643 on (B, C and D) are shown. ($K_v11.1a$; $K_v11.1b$; $K_v11.1a/K_v11.1b$: n = 9; 12; 7).

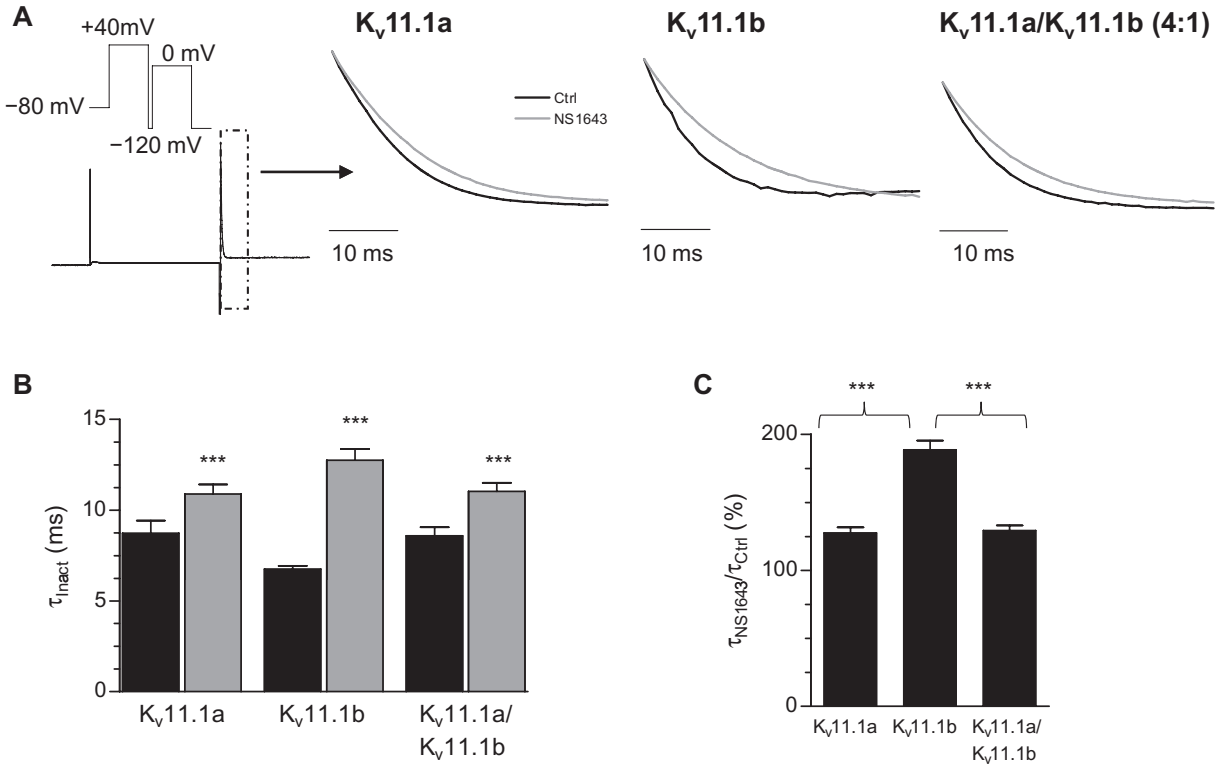

Figure 4

Effect of NS1643 on inactivation kinetics of K_v11.1 channels. Oocytes expressing K_v11.1a (left panel), K_v11.1b (middle panel) or K_v11.1a/K_v11.1b (4:1) (right panel) were voltage clamped at +40 mV for 1 s and stepped to −120 mV for 10 ms (K_v11.1a and K_v11.1a/K_v11.1b) or 5 ms (K_v11.1b) to allow the channels to recover from inactivation, and subsequently clamped at 0 mV to investigate the time-course of inactivation. Representative traces of K_v11.1a are shown in (A, left). Also shown in (A) are enlargements of the time-course of inactivation normalized to maximum current amplitude for K_v11.1a, K_v11.1b and K_v11.1a/K_v11.1b (4:1) respectively. (B) The time-course of inactivation was well-fit by a single exponential function. Time constants of inactivation are shown in (B), and the relative effect of NS1643 in (C). (K_v11.1a; K_v11.1b; K_v11.1a/K_v11.1b: n = 10; 11; 6).

enlargements of the initial rising phase of representative currents recorded under control conditions and in the presence of NS1643 are shown for K_v11.1a (left side), K_v11.1b (middle) and K_v11.1a/K_v11.1b (right side). The dotted lines correspond to the fit of the deactivation process extrapolated back to the point where the command voltage was changed from +40 to −60 mV. To avoid any potential influence of fast deactivation, especially for K_v11.1b, on the recovery kinetics, the recorded current was subtracted from the extrapolated values to obtain the true time-course of recovery. In Figure 5B, the resulting (difference) currents are shown. The currents were normalized to maximum amplitude for comparison of the time-course. NS1643 changed the time-course of recovery only a little for K_v11.1a and K_v11.1a/K_v11.1b channels, while a clear slowing of the process was observed for K_v11.1b. Data for the time constant of recovery ($\tau_{recovery}$) are shown in Figure 5C. The data show that for K_v11.1a and K_v11.1a/K_v11.1b, NS1643 induced a small, but significant increase in $\tau_{recovery}$ ($P < 0.001$ and $P < 0.001$, respectively), while for K_v11.1b the increase ($P < 0.001$) was more noticeable. Comparing the relative change in $\tau_{recovery}$, the effect of NS1643 is clearly more noticeable for K_v11.1b than for K_v11.1a or K_v11.1a/K_v11.1b ($P < 0.001$ and $P < 0.001$ respectively).

Effects of RPR260243 on K_v11.1 channels

Having investigated a compound with a relative broad mechanism of action, we turned to the K_v11.1 activator RPR260243, a compound which has been reported to primarily affect deactivation kinetics (Kang *et al.*, 2005). The effects of 10 μM RPR260243 on the K_v11.1 isoforms are illustrated in Figure 6. From the *I*/*V* relationships in the absence and presence of RPR260243, it can be observed that RPR260243 increased the steady-state current of K_v11.1a homomers and K_v11.1a/ K_v11.1b (4:1) heteromers, whereas it had no effect on Kv11.1b steady-state current (Figure 6A,B). This was also observed for higher concentrations of RPR260243 (Supporting Information Figure S3). For both homomeric

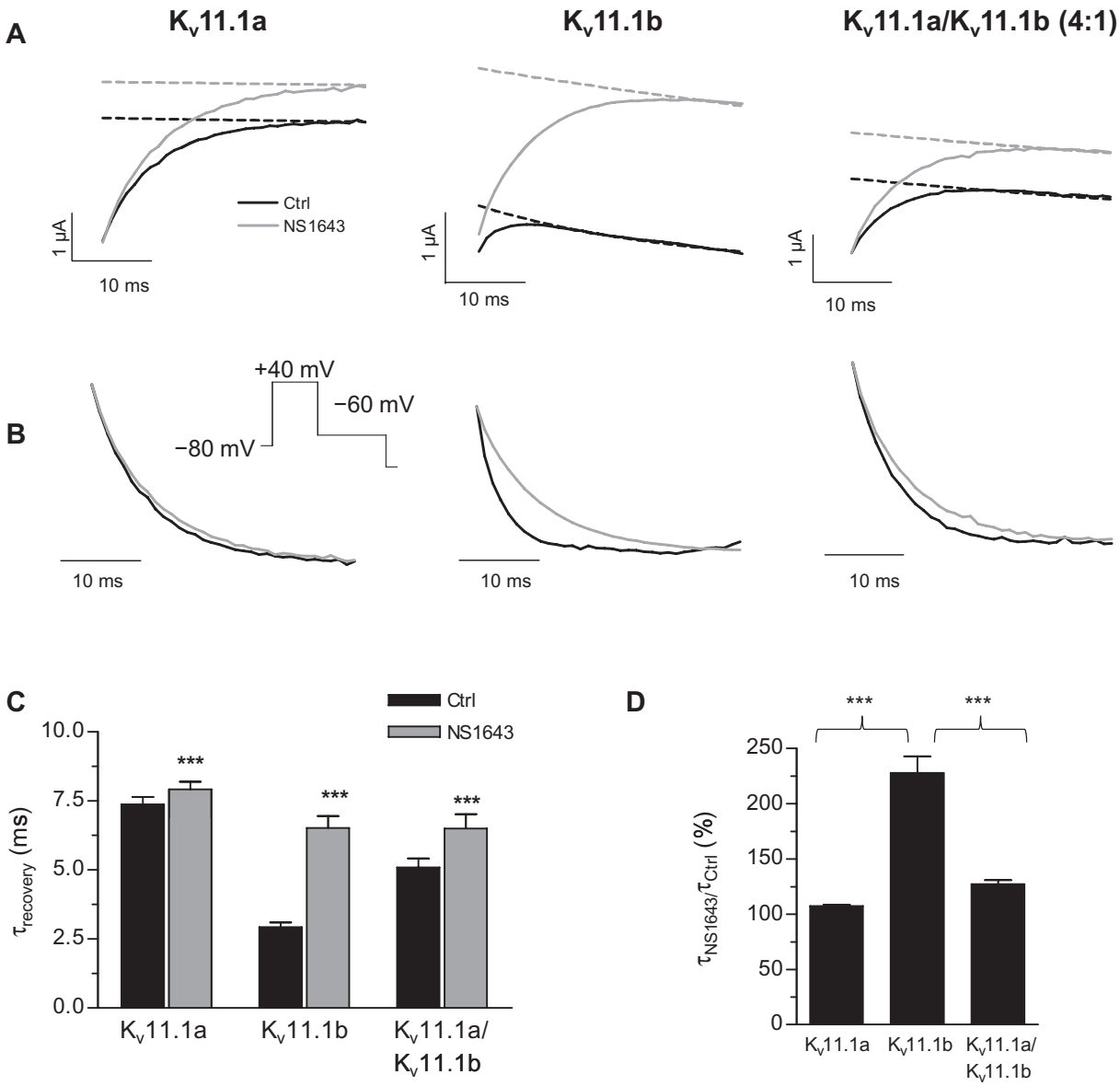

Figure 5

Effect of NS1643 on kinetics of recovery from inactivation of $K_v11.1$ channels. (A) Representative current trace of the recovery from inactivation from *Xenopus laevis* oocytes expressing $K_v11.1a$ (left panel), $K_v11.1b$ (middle panel) or $K_v11.1a/K_v11.1b$ (4:1) (right panel) in the absence and presence of 30 µM NS1643. The fit of the deactivation (dotted line) was extrapolated to the time-point when the membrane potential was changed from +40 to −60 mV. By subtracting the initial rising phase of the current from the extrapolated fit of deactivation, the time-course of the recovery from inactivation can be isolated (B). A single-exponential function was fitted to the isolated time-course of recovery from inactivation. The resulting time constants of recovery from inactivation are shown in (C), and the relative effect of NS1643 in (D). ($K_v11.1a$; $K_v11.1b$; $K_v11.1a/K_v11.1b$: n = 10; 13; 7).

and heteromeric channels, RPR260243 had no significant effect on the voltage dependence of activation (Figure 6C). Likewise, RPR260243 had no effect on the kinetics of inactivation or recovery from inactivation (data not shown). However, it did cause a slight but significant slowing of activation for $K_v11.1a$ [τ_{act}: 189 ± 14 ms (control) vs. 209 ± 14 ms, $P < 0.01$], but not for $K_v11.1b$ [τ_{act}: 143 ± 13 ms (control) vs. 148 ± 17 ms, P = ns] or $K_v11.1a/K_v11.1b$ [τ_{act}: 166 ± 15 ms (control) vs. 166 ± 10 ms, P = ns].

From the representative current traces in Figure 6A, it can be observed that RPR260243 has noticeable effects on deactivation kinetics. On both channel isoforms, RPR260243 caused a concentration-dependent slowing of deactivation (Supporting Information Figure S3). To further investigate the effect of RPR260243 on deactivation

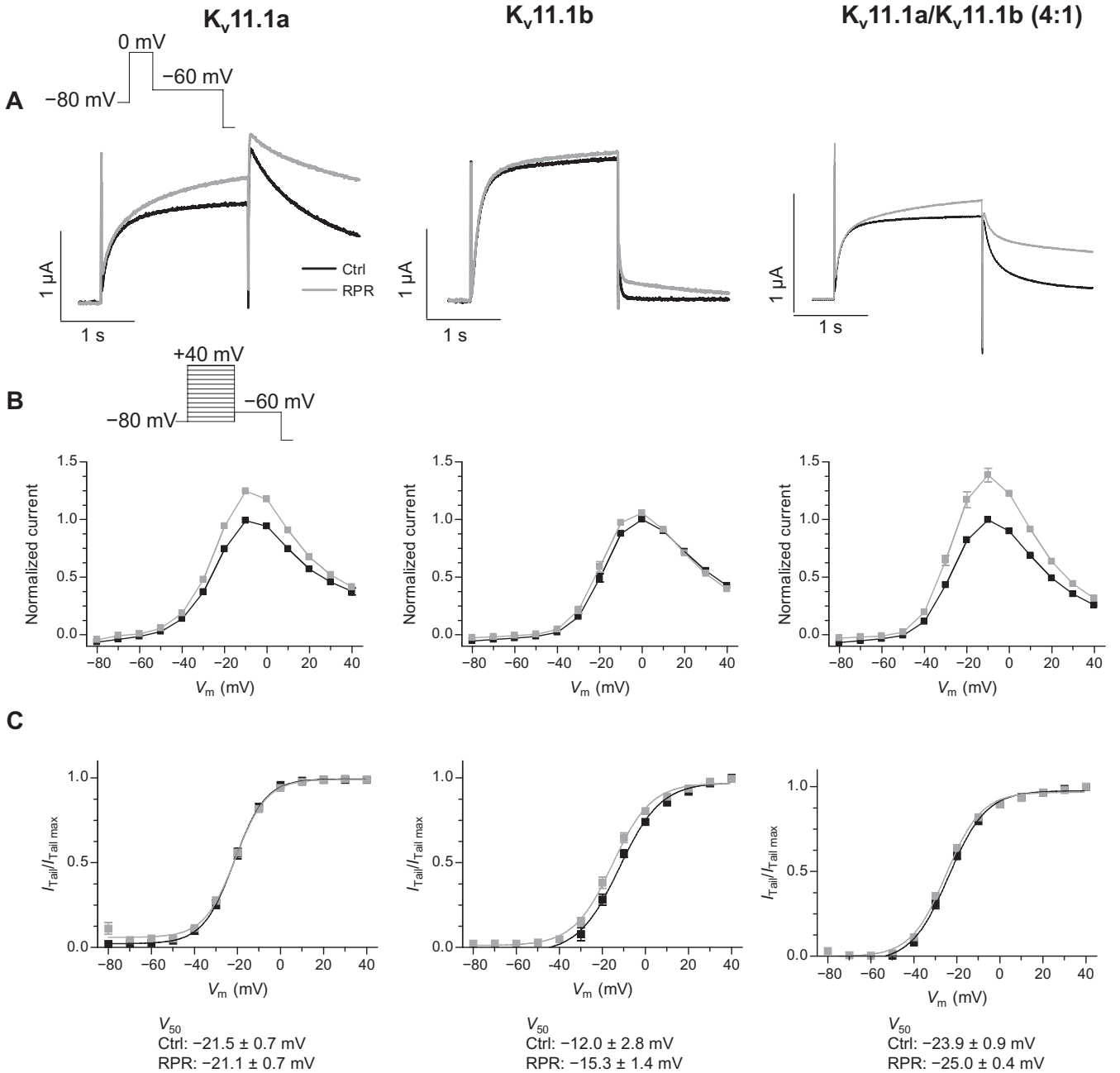

Figure 6

Effect of RPR260243 on current–voltage relationships of $K_v11.1$ channels. (A) Representative current traces recorded at a test potential of 0 mV from *Xenopus laevis* oocytes expressing $K_v11.1a$ (left panel), $K_v11.1b$ (middle panel) or $K_v11.1a/K_v11.1b$ (4:1) (right panel) in the absence and presence of RPR260243 (10 µM). Normalized current–voltage relationships (B) and voltage dependence of activation (C) before and after application of RPR260243 (for further details, see Figure 1). ($K_v11.1a$; $K_v11.1b$; $K_v11.1a/K_v11.1b$: $n = 7; 7; 9$).

kinetics, we fitted the time-course of deactivation measured at −60 mV to a double-exponential function. The time constant of the slow component of deactivation (τ_{slow}) was significantly increased for both homomeric and heteromeric channels after RPR260243. The relative effect of RPR260243 on τ_{slow} was significantly greater on $K_v11.1b$ compared to $K_v11.1a$ and $K_v11.1a/K_v11.1b$ ($P < 0.001$ and $P < 0.001$, respectively) (Figure 7B, right panel). The marked effect of RPR260243 on the slow time constant for Kv11.1 is also noticeable from the enlargement of the time-course of deactivation in Figure 7A (middle panel). Similarly, the time constant of the fast component of deactivation (τ_{fast}) was significantly increased for $K_v11.1b$ and $K_v11.1a/K_v11.1b$ after application of RPR260243. In addition, the

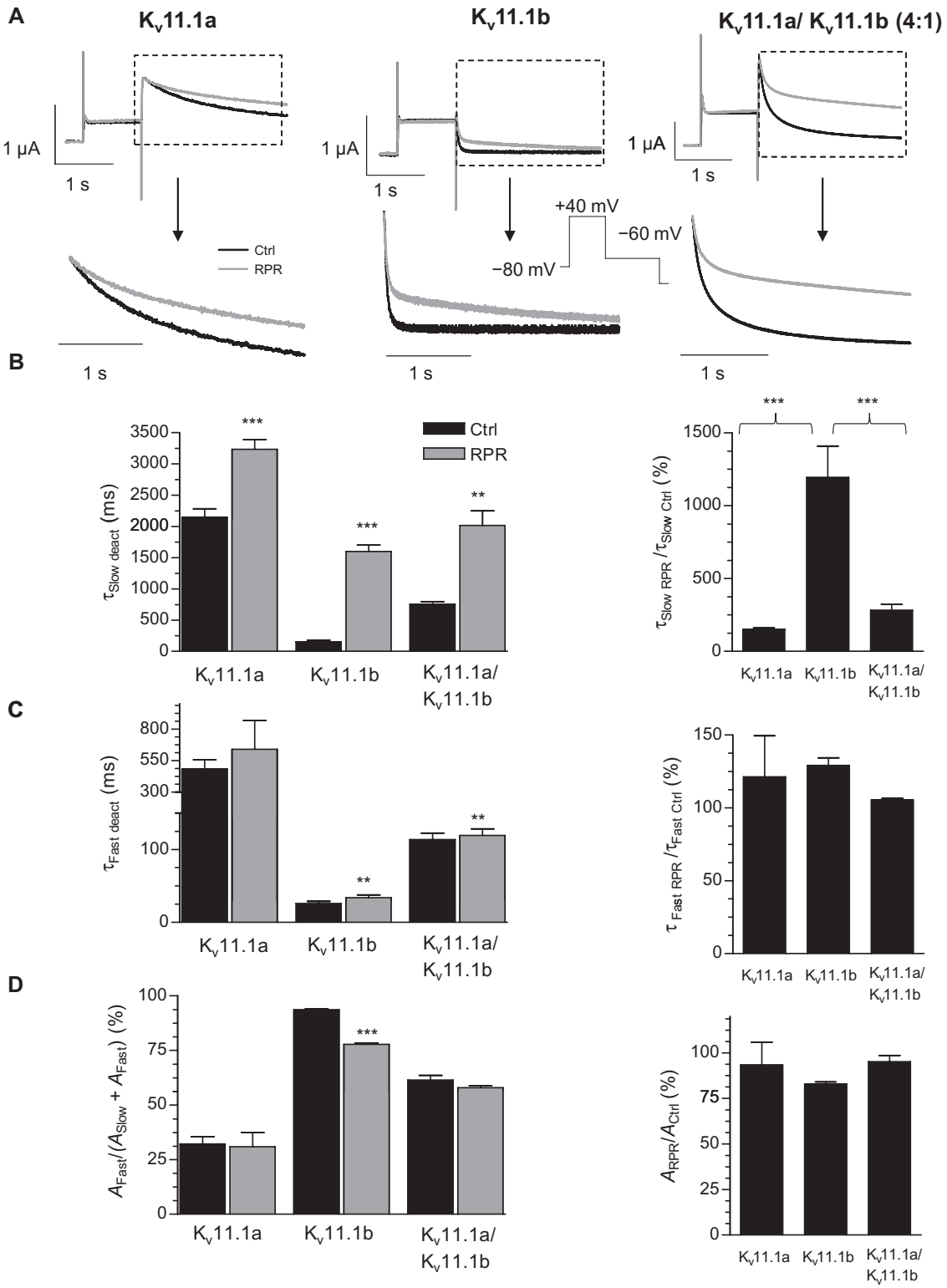

Figure 7

Effect of RPR260243 on deactivation kinetics of K_v11.1 channels. Representative current traces from oocytes expressing K_v11.1a (left panel), K_v11.1b (middle panel) or K_v11.1a/K_v11.1b (4:1) (right panel) in the absence and presence of RPR260243 are shown in the top panel, and an enlargement of the tail currents (normalized to maximum current amplitude) is shown in the bottom panel. Time constants of the slow component (B), fast component (C) and the relative contribution of the fast and slow component (D) before and after RPR260243 (10 µM) are shown. In addition, the relative effect of RPR260243 on (B, C and D) are shown (for further explanation, see Figure 3). (K_v11.1a; K_v11.1b; K_v11.1a/K_v11.1b: n = 5; 6; 8).

relative contribution of the fast component of deactivation significantly decreased after application of RPR260243 for $K_v11.1b$ (Figure 7D).

Discussion and conclusions

In this study, we have investigated two $K_v11.1$ activators NS1643 and RPR260243, which represent two compounds with marked differences in channel activation mechanisms. Previously, the effects of these compounds have only been characterized on the $K_v11.1a$ isoform (Kang *et al.*, 2005; Casis *et al.*, 2006; Hansen *et al.*, 2006a; Perry *et al.*, 2007; Xu *et al.*, 2008). However, at least two isoforms of $K_v11.1$ have been found to be co-expressed in native tissues (Ohya *et al.*, 2002; Jones *et al.*, 2004; Guasti *et al.*, 2005). To determine whether NS1643 and RPR260243 have differential effects on $K_v11.1$ isoforms, we compared the effects of these compounds on $K_v11.1a$ and $K_v11.1b$ channels. Except for a shorter but unique N-terminus, $K_v11.1a$ and $K_v11.1b$ are identical (Lees-Miller *et al.*, 1997; London *et al.*, 1997). In general, homomeric $K_v11.1b$ channels display faster kinetics than $K_v11.1a$ channels (Larsen *et al.*, 2008).

In agreement with earlier studies (Kang *et al.*, 2005; Casis *et al.*, 2006; Hansen *et al.*, 2006a; Perry *et al.*, 2007; Xu *et al.*, 2008), we found that NS1643 enhanced $K_v11.1a$ currents primarily by slowing the rates of deactivation and inactivation, while RPR260243 acted mainly by slowing the rate of deactivation. In general, both NS1643 and RPR260243 affected the same biophysical properties of $K_v11.1b$ as they did of $K_v11.1a$. However, for both activators, the magnitudes of the effects were found to be isoform dependent. NS1643 was found to have higher efficacy on $K_v11.1b$ compared to $K_v11.1a$ steady-state currents. The greater efficacy of NS1643 on $K_v11.1b$ channels was partly explained by approximately twofold greater increases in the time constants of $K_v11.1b$ deactivation, inactivation and recovery from inactivation processes as compared to $K_v11.1a$. Similarly, the relative effect of RPR260243 on deactivation kinetics was more marked on the $K_v11.1b$ isoform, showing a ~10-fold greater decrease of the slow time constant for $K_v11.1b$ compared to the $K_v11.1b$ isoform.

Both NS1643 and RPR260243 have been suggested to bind in or near the channel pore (Perry *et al.*, 2007; Xu *et al.*, 2008). Importantly, by applying NS1643 from either the intra- or extracellular side of the membrane of *X. laevis* oocytes expressing $K_v11.1a$ channels, Xu *et al.* (2008) showed that NS1643 interacts with the extracellular region of the pore. In contrast, RPR260243 interacts with the pore from the intracellular side as demonstrated by mutational analysis and computational docking studies (Perry *et al.*, 2007). This difference in binding sites may underlie the selective effect of RPR260243 on deactivation kinetics. In addition, a third $K_v11.1$ activator PD307243 has also been found to interact with the channel pore (Xu *et al.*, 2008). The region surrounding the channel pore of $K_v11.1$ therefore appears to be the preferred binding site for $K_v11.1$ activators. As this region is identical between all described $K_v11.1$ isoforms (Warmke and Ganetzky, 1994; Lees-Miller *et al.*, 1997; London *et al.*, 1997; Kupershmidt *et al.*, 1998; Guasti *et al.*, 2008; Huffaker *et al.*, 2009), it may, from a structural point of view, seem difficult to achieve isoform selectivity. Nevertheless, our data suggest that at least some degree of selectivity can be achieved by differentially targeting specific kinetic processes inherently different between the isoforms.

The structural basis for the differential effects of NS1643 and RPR260243 on $K_v11.1a$ and $K_v11.1b$ is unclear. Perry *et al.* (2009) recently reported that the effect of PD118057, another $K_v11.1$ activator that also binds in the pore region, was greatly increased by mutation of residues C643 and M645 in the S6 helix of $K_v11.1a$. Results from a molecular docking model suggested that both mutations reduced steric hindrance for drug binding. By analogy, it can be hypothesized that interactions between the long N-terminal of $K_v11.1a$ and the pore region to some degree alter the structure of the binding sites, and thereby restrict NS1643 and RPR260243 from accessing their optimal binding configuration. Consequently, in $K_v11.1b$ channels, the long N-terminal is absent and the compounds have easier access to their binding sites. This mechanism would, however, be expected to also affect the EC_{50} value unless association and dissociation rates are changed to a similar extent. We were not able to obtain EC_{50} values for RPR260243 (see Methods), but for NS1643 the EC_{50} was not different on $K_v11.1a$ and $K_v11.1b$ channels. An alternative hypothesis could be that while the N-terminal of $K_v11.1a$ does not restrict the compounds from binding to the channel *per se*, it may restrict the movements of the channel complex by stabilizing channel states. Such an effect would also explain the inherent differences in kinetics between $K_v11.1a$ and $K_v11.1b$ channels (Larsen *et al.*, 2008). Following this hypothesis, NS1643 and RPR260243 would be able to induce greater conformational changes in $K_v11.1b$ channels than in $K_v11.1a$ channels where the long N-terminal restricts the movements. This hypothesis needs to be addressed in future studies.

The effect of $K_v11.1$ activators will probably be dependent on the distribution of $K_v11.1$ isoforms

in a given tissue and whether the isoforms form heteromeric channel complexes in that tissue. Endogenous co-expression of K_v11.1a and K_v11.1b has been described in heart, brain and smooth muscle (Ohya *et al.*, 2002; Jones *et al.*, 2004; Guasti *et al.*, 2005). From mRNA levels, it has been found that the human heart left ventricle contains on average 10–20% K_v11.1b (Larsen *et al.*, 2008). Consequently, differential expression of K_v11.1 isoforms should be taken into consideration when developing and investigating novel K_v11.1 activators. To address this issue, the effects of NS1643 and RPR260243 were investigated on heteromeric K_v11.1a/K_v11.1b channels. Work from our group has shown that the kinetic properties of heteromeric K_v11.1a/K_v11.1b macroscopic currents are dependent on the relative abundance of the isoforms (Larsen *et al.*, 2008; Larsen and Olesen, 2010). Accordingly, we observed that heteromeric expression resulted in currents intermediate of those observed for homomeric K_v11.1a and K_v11.1b channels. Comparison of the deactivation kinetics of homomeric channels and the resulting kinetics of the co-expressed channels strongly suggested that heteromeric channel formation did occur. When co-expressed in a molar ratio of 4:1 (K_v11.1a/K_v11.1b), the effects of both NS1643 and RPR260243 were similar to the effects seen for homomeric K_v11.1a channels. If the hypothesis that interaction between the K_v11.1a-type N-terminal with the pore domain restricts the conformational changes that can be induced by binding of an activator is true, the presence of K_v11.1a N-terminals in a heteromeric channel is likely to determine the efficacy of the activators. The observed effects of NS1643 and RPR260243 on co-expressed channels are in agreement with such a hypothesis.

Recently, Huffaker *et al.* (2009) described a link between schizophrenia and up-regulation of a brain-specific fast-deactivating K_v11.1 isoform (KCNH2-3.1). The up-regulation of the fast-deactivating isoform leads to increased excitability in primary cortical neurones. In theory, a targeted gating modifier may convert a fast-deactivating K_v11.1 channel isoform to a more K_v11.1a-like phenotype, thereby reducing excitability to non-pathological levels. The differential effects of two K_v11.1 channel activators, especially RPR260243, on deactivation properties that we observed in this study suggest that this would indeed be a possibility. Although the effect of K_v11.1 activators has not been tested on the KCNH2-3.1 isoform, our data suggest that in principle a fast-deactivating isoform (K_v11.1b) can be converted to a more K_v11.1a-like phenotype. The use of differentially acting K_v11.1 activators may represent a novel treatment of diseases caused by changes in the abundance of K_v11.1 isoforms.

A limitation to our study is that we did not perform computational modelling to verify that the effects of NS1643 and RPR260243 on Kv11.1 currents can be fully represented by the observed changes in kinetic rates. Therefore, we cannot completely rule out the possibility that changes in surface density of the channels during drug application may also play a role.

In conclusion, we demonstrated that two previously described activators on K_v11.1a channels have qualitatively similar effects on K_v11.1b channels. However, the efficacy of the activators is isoform dependent. Our results suggest that development of isoform-selective activators might be possible, and highlight the importance of the N-terminus in gating of K_v11.1 channels. Furthermore, the demonstration of isoform-dependent effects of K_v11.1 activators stresses the importance of establishing the relative abundance of isoforms in the targeted tissue and investigating the effect of activators on the relevant combination of K_v11.1 isoforms.

Acknowledgements

Synthesis of NS1643 and RPR260243 by Joachim Demnitz is highly appreciated. This work was supported by the Danish National Research Foundation, The Novo Nordisk Foundation and The Aase and Ejnar Danielsen Foundation. Trine Christensen is acknowledged for technical assistance.

Conflict of interest

M.G. is an employee at NeuroSearch A/S.

References

Alexander SP, Mathie A, Peters JA (2008). *Guide to Receptors and Channels (GRAC)*, 3rd edition. Br J Pharmacol 153 (Suppl. 2): S1–S209.

Casis O, Olesen SP, Sanguinetti MC (2006). Mechanism of action of a novel human ether-a-go-go-related gene channel activator. Mol Pharmacol 69: 658–665.

Chiesa N, Rosati B, Arcangeli A, Olivotto M, Wanke E (1997). A novel role for HERG K^+ channels: spike-frequency adaptation. J Physiol 501: 313–318.

Diness TG, Yeh YH, Qi XY, Chartier D, Tsuji Y, Hansen RS *et al.* (2008). Antiarrhythmic properties of a rapid delayed-rectifier current activator in rabbit models of acquired long QT syndrome. Cardiovasc Res 79: 61–69.

Farrelly AM, Ro S, Callaghan BP, Khoyi MA, Fleming N, Horowitz B *et al.* (2003). Expression and function of KCNH2 (HERG) in the human jejunum. Am J Physiol Gastrointest Liver Physiol 284: G883–G895.

Guasti L, Cilia E, Crociani O, Hofmann G, Polvani S, Becchetti A *et al.* (2005). Expression pattern of the ether-a-go-go-related (ERG) family proteins in the adult mouse central nervous system: evidence for coassembly of different subunits. J Comp Neurol 491: 157–174.

Guasti L, Crociani O, Redaelli E, Pillozzi S, Polvani S, Masselli M *et al.* (2008). Identification of a posttranslational mechanism for the regulation of hERG1 K^+ channel expression and hERG1 current density in tumor cells. Mol Cell Biol 28: 5043–5060.

Hansen RS, Diness TG, Christ T, Demnitz J, Ravens U, Olesen SP *et al.* (2006a). Activation of human ether-a-go-go-related gene potassium channels by the diphenylurea 1,3-bis-(2-hydroxy-5-trifluoromethyl-phenyl)-urea (NS1643). Mol Pharmacol 69: 266–277.

Hansen RS, Diness TG, Christ T, Wettwer E, Ravens U, Olesen SP *et al.* (2006b). Biophysical characterization of the new human ether-a-go-go-related gene channel opener NS3623 [*N*-(4-bromo-2-(1H-tetrazol-5-yl)-phenyl)-*N*′-(3′-trifluoromethylphenyl)urea]. Mol Pharmacol 70: 1319–1329.

Hansen RS, Olesen SP, Grunnet M (2007). Pharmacological activation of rapid delayed rectifier potassium current suppresses bradycardia-induced triggered activity in the isolated guinea pig heart. J Pharmacol Exp Ther 321: 996–1002.

Huffaker SJ, Chen J, Nicodemus KK, Sambataro F, Yang F, Mattay V *et al.* (2009). A primate-specific, brain isoform of KCNH2 affects cortical physiology, cognition, neuronal repolarization and risk of schizophrenia. Nat Med 15: 509–518.

Jespersen T, Grunnet M, Angelo K, Klaerke DA, Olesen SP (2002). Dual-function vector for protein expression in both mammalian cells and *Xenopus laevis* oocytes. Biotechniques 32: 536–540.

Jones EM, Roti Roti EC, Wang J, Delfosse SA, Robertson GA (2004). Cardiac IKr channels minimally comprise hERG 1a and 1b subunits. J Biol Chem 279: 44690–44694.

Kang J, Chen XL, Wang H, Ji J, Cheng H, Incardona J *et al.* (2005). Discovery of a small molecule activator of the human ether-a-go-go-related gene (HERG) cardiac K^+ channel. Mol Pharmacol 67: 827–836.

Kupershmidt S, Snyders DJ, Raes A, Roden DM (1998). A K^+ channel splice variant common in human heart lacks a C-terminal domain required for expression of rapidly activating delayed rectifier current. J Biol Chem 273: 27231–27235.

Larsen AP, Olesen SP (2010). Differential expression of hERG1 channel isoforms reproduces properties of native I(Kr) and modulates cardiac action potential characteristics. PLoS ONE 5: e9021.

Larsen AP, Olesen SP, Grunnet M, Jespersen T (2008). Characterization of hERG1a and hERG1b potassium channels-a possible role for hERG1b in the I (Kr) current. Pflugers Arch 456: 1137–1148.

Lees-Miller JP, Kondo C, Wang L, Duff HJ (1997). Electrophysiological characterization of an alternatively processed ERG K^+ channel in mouse and human hearts. Circ Res 81: 719–726.

London B, Trudeau MC, Newton KP, Beyer AK, Copeland NG, Gilbert DJ *et al.* (1997). Two isoforms of the mouse ether-a-go-go-related gene coassemble to form channels with properties similar to the rapidly activating component of the cardiac delayed rectifier K^+ current. Circ Res 81: 870–878.

Ohya S, Horowitz B, Greenwood IA (2002). Functional and molecular identification of ERG channels in murine portal vein myocytes. Am J Physiol Cell Physiol 283: C866–C877.

Perry M, Sachse FB, Sanguinetti MC (2007). Structural basis of action for a human ether-a-go-go-related gene 1 potassium channel activator. Proc Natl Acad Sci USA 104: 13827–13832.

Perry M, Sachse FB, Abbruzzese J, Sanguinetti MC (2009). PD-118057 contacts the pore helix of hERG1 channels to attenuate inactivation and enhance K^+ conductance. Proc Natl Acad Sci USA 106: 20075–20080.

Sanguinetti MC, Jiang C, Curran ME, Keating MT (1995). A mechanistic link between an inherited and an acquired cardiac arrhythmia: HERG encodes the IKr potassium channel. Cell 81: 299–307.

Trudeau MC, Warmke JW, Ganetzky B, Robertson GA (1995). HERG, a human inward rectifier in the voltage-gated potassium channel family. Science 269: 92–95.

Warmke JW, Ganetzky B (1994). A family of potassium channel genes related to eag in *Drosophila* and mammals. Proc Natl Acad Sci USA 91: 3438–3442.

Xu X, Recanatini M, Roberti M, Tseng GN (2008). Probing the binding sites and mechanisms of action of two human ether-a-go-go-related gene channel activators, 1,3-bis-(2-hydroxy-5-trifluoromethyl-phenyl)-urea (NS1643) and 2-[2-(3,4-dichloro-phenyl)-2,3-dihydro-1H-isoindol-5-ylamino]-nicotinic acid (PD307243). Mol Pharmacol 73: 1709–1721.

Zhou J, Augelli-Szafran CE, Bradley JA, Chen X, Koci BJ, Volberg WA *et al.* (2005). Novel potent human ether-a-go-go-related gene (hERG) potassium channel enhancers and their *in vitro* antiarrhythmic activity. Mol Pharmacol 68: 876–884.

Supporting information

Additional Supporting Information may be found in the online version of this article:

Figure S1 Comparison of deactivation kinetics of experimental and theoretical currents. The theoretical current decay was calculated under the assumption that only homomeric K_v11.1a and K_v11.1b channels were formed in a 4:1 ratio. The experimental current decay was calculated from the observed macroscopic deactivation properties of oocytes expression K_v11.1a/K_v11.1b in a 4:1 ratio (Figures 3 and 7).

Figure S2 Concentration–response relationship of NS1643 for K_v11.1a (left) and K_v11.1b (right). (A) Current traces in the absence or presence of 10 and 100 μM NS1643. (B) Concentration–response curve for K_v11.1a and K_v11.1b. EC_{50} values were calculated from individual sigmoidal fits to the normalized steady-state current measured at 0 mV as a function of increasing concentrations of NS1643. (K_v11.1a; K_v11.1b: n = 5; 5).

Figure S3 Concentration–response relationship of RPR260243 for K_v11.1a (left) and K_v11.1b (right). (A) Representative current traces recorded at a test potential of 0 mV in the absence and presence of 10 and 100 μM RPR260243.

Please note: Wiley-Blackwell are not responsible for the content or functionality of any supporting materials supplied by the authors. Any queries (other than missing material) should be directed to the corresponding author for the article.